High Pressure Bulk Synthesis of Crystalline C6N9H3·HCl: A Novel C3N4 Graphitic Derivative

6 AUTHORS, INCLUDING:

Laurence AJ Garvie
Arizona State University
109 PUBLICATIONS **1,752** CITATIONS

SEE PROFILE

Paul F. McMillan
University College London
404 PUBLICATIONS **11,611** CITATIONS

SEE PROFILE

High-Pressure Bulk Synthesis of Crystalline $C_6N_9H_3$·HCl: A Novel C_3N_4 Graphitic Derivative

Zhihong Zhang, Kurt Leinenweber, Matt Bauer, Laurence A. J. Garvie, Paul F. McMillan, and George H. Wolf*

Contribution from the Materials Research Science and Engineering Center, Arizona State University, Tempe, Arizona 85287

Received February 12, 2001

Abstract: A novel carbon nitride compound, structurally related to the proposed graphitic phase of C_3N_4, has been synthesized in a bulk well-crystallized form. The new material, with stoichiometry $C_6N_9H_4Cl$, was prepared through a solid-state reaction of 2,4,6-triamino-1,3,5-triazine with 2,4,6-trichloro-1,3,5-triazine at 1.0−1.5 GPa and 500−550 °C and also through a self-reaction of 2-amino-4,6-dichloro-1,3,5-triazine at similar conditions. X-ray and electron diffraction measurements on the yellowish compound indicate a hexagonal space group ($P6_3$/m) with cell parameters of $a = 8.4379(10)$ Å and $c = 6.4296(2)$ Å. This new compound possesses a two-dimensional $C_6N_9H_3$ framework that is structurally related to the hypothetical $P6$m2 graphitic phase of C_3N_4, but with an ordered arrangement of C_3N_3 voids. The large voids in the graphene sheets are occupied by chloride ions with an equivalent number of nitrogen atoms on the framework protonated for charge balance. The composition of the sample was determined by bulk chemical analysis and confirmed by electron energy loss (EELS) spectroscopy. The chemical and structural model is consistent with bulk density measurements and with the infrared and ^{13}C NMR spectra. This work represents the first bulk synthesis of a well-characterized and highly crystalline material containing a continuous network of alternating carbon and nitrogen atoms.

Introduction

A great deal of theoretical and experimental activity has been directed toward the possibility of developing new carbon nitride materials with a hardness that may rival or even exceed that of diamond. Several hypothetical carbon nitrides with stoichiometry C_3N_4 have been at the focus of this search for superhard materials. Cohen et al.[1] first suggested that a C_3N_4 phase, isostructural to the technologically important β-Si_3N_4, could be less compressible than diamond. This early conjecture, made on the basis of an empirical scaling law, was later supported by more detailed first-principles calculations which indicate that the bulk modulus of the hypothetical β-C_3N_4 phase would be comparable to that of diamond.[2]

With further theoretical work, several other high-density low-compressibility forms of C_3N_4 have been proposed, all of which are based on 4,3 networks where the carbon atoms are in tetrahedral coordination with nitrogen and the nitrogen atoms are in trigonal coordination with carbon.[3,4] In particular, an α-form of C_3N_4, isostructural to α-Si_3N_4, is actually predicted to be more stable than the β-form at all pressures.[4] More recently, model structures with a cubic $I43d$ symmetry[4] and a pseudocubic defective zinc blende symmetry ($P43m$ symmetry)[3,4] have been proposed as possible dense low compressibility forms of C_3N_4. Although these proposed phases are energetically less stable than the α and β forms at ambient pressure, calculations suggest that they may be accessible in high-pressure synthesis experiments and recoverable upon pressure release.[3,4]

In similarity to the pure carbon system, it is likely that at ambient conditions a graphitic form of C_3N_4 would be more stable than any of the tetrahedral-based low-compressibility phases. Indeed, first-principles calculations do predict that some planar forms of C_3N_4 are relatively more stable, though only marginally, to the α and β phases at ambient pressure.[3−7] By analogy with the high-pressure synthesis of diamond from graphite, a carbon nitride graphitic phase could be an ideal precursor for the formation of bulk high-density carbon nitrides through high-pressure treatment.

A bulk synthesis of well-characterized C_3N_4 in any structural form has been elusive, largely due to the high thermodynamic activity of nitrogen in these compounds and the tendency to form molecular nitrogen even at only moderately elevated temperatures.[8] There have been numerous claims of the syntheses of microcrystalline forms of the low-compressibility phases of C_3N_4. The majority of the synthetic methods are based on thin film growth which employed various physical and chemical vapor deposition methods.[9−16] Nanocrystalline carbon nitride phases have also been claimed in catalyzed decomposi-

(1) Cohen, M. L. *Phys. Rev.* **1985**, *B32*, 7988.
(2) Liu, A. L.; Cohen, M. L. *Science* **1989**, *245*, 841.
(3) Liu, A. Y.; Wentzcovitch, R. M. *Phys. Rev. B* **1994**, *50*, 10362−10365.
(4) Teter, D. M.; Hemley, R. J. *Science* **1996**, *271*, 53.

(5) Ortega, J.; Sankey, O. F. *Phys. Rev. B* **1995**, *51*, 2624−2627.
(6) Miyamoto, Y.; Cohen, M. L.; Louie, S. G. *Solid State Commun.* **1997**, *102*, 605.
(7) Lowther, J. E. *Phys. Rev. B* **1999**, *59*, 11683−11686.
(8) Badding, J. V.; Nesting, D. C. *Chem. Mater.* **1996**, *8*, 535−540.
(9) Niu, C.; Lu, Y. Z.; Lieber, C. M. *Science* **1993**, *261*, 334.
(10) Yu, K. M.; Cohen, M. L.; Haller, E. E.; Hansen, W. L.; Liu, A. Y.; Wu, I. C. *Phys. Rev. B* **1994**, *49*, 5034−5037.
(11) Narayan, J.; Reddy, J.; Biunno, N.; Kanetkar, S. M.; Tiwari, P.; Parikh, N. *Mater. Sci. Eng.* **1994**, *26*, 49.
(12) Ren, Z.-M.; Du, Y.-C.; Qiu, Y.; Wu, J.-D.; Ying, Z.-F.; Xiong, X.-X.; Li, F.-M. *Phys. Rev. B* **1995**, *51*, 5274−5277.
(13) Zhang, Z. J.; Fan, S.; Lieber, C. M. *Appl. Phys. Lett.* **1995**, *66*, 3582.
(14) Tabbal, M.; Merel, P.; Moisa, S.; Chaker, M.; Ricard, A.; Moisan, M. *Appl. Phys. Lett.* **1996**, *69*, 1698.
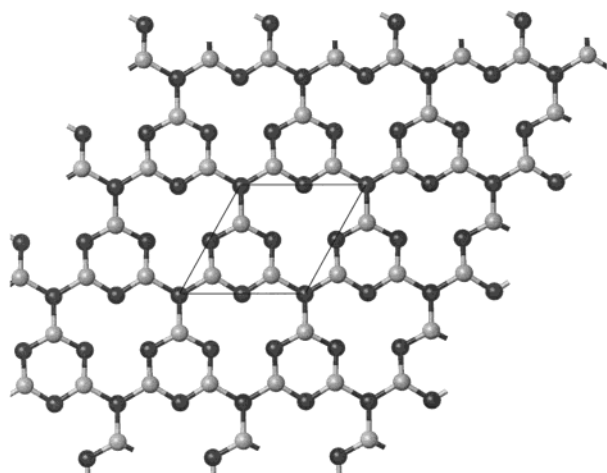
Figure 1. Basal plane structure for the hypothetical "fully densified" graphitic phase of C_3N_4; the projection view is perpendicular to the *c* axis. The gray spheres represent carbon and the black spheres nitrogen. The hexagonal ordering of C voids in a CN network results in a basal unit cell that is dimensionally 2 times larger than that of hexagonal graphite.

tion products of various organic precursors.[17,18] In all of these cases the samples are difficult to characterize since the product material is highly heterogeneous and the nano- or microcrystalline CN-rich phases comprise only a small fraction of the bulk. Moreover, the diffraction evidence that is typically presented is less than convincing because significant discrepancies exist between the measured diffraction patterns and those calculated using the model structures.[19]

Kouvetakis et al.[20] were successful in synthesizing X-ray amorphous homogeneous thin films with an approximate C_3N_4 composition through a relatively moderate temperature (400–500 °C) decomposition of substituted aminotriazine-based unimolecular carbon nitride precursors. The authors proposed a structure of the amorphous carbon nitride based on planar graphene sheets of alternately bonded C and N atoms (see Figure 1). The graphene sheets contain a periodic hexagonal array of carbon voids in a hypothetical CN network. The sheets consist of two types of nitrogen atoms, one in 2-fold coordination within the triazine rings and the other in 3-fold coordination connecting three C_3N_3 heterocycle rings. All of the carbon atoms are sp² hybridized and in 3-fold coordination with nitrogen. Subsequent attempts to synthesize high-density forms of carbon nitride from high-pressure treatment of similar materials has thus far yielded inconclusive results.[21]
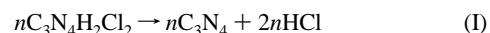
Recently, Demazeau et al.[22] reported the synthesis of a bulk crystalline graphitic-like phase with C_3N_4 composition through a molecular solvothermal route under pressure. In their method, melamine (2,4,6-triamine-1,3,5-triazine) was reacted with cyanuric chloride (2,4,6-trichloro-1,3,5-triazine) in the presence of

a nucleophilic amino base, either triethylamine (pK_b 3.25) or diisopropylethylamine, under modest pressures (130 MPa) at temperatures of only 250 °C (see also ref 23). Their sample, however, was only poorly crystalline and only a single broad X-ray reflection was observed at approximately 3.27 Å. Moreover, chemical analysis of their product revealed a significant contamination by both chlorine and hydrogen. In subsequent work a bulk material with a higher degree of crystallinity but similar C/N ratio was prepared at higher pressures and temperatures (3 GPa and 800–840 °C) from melamine in the presence of hydrazine (NH_2NH_2) as a nitriding agent.[24] For this material, a strong diffraction peak was observed at 3.17 Å and three weaker peaks were observed at 3.3, 2.0, and 1.6 Å. The authors were not able to index their diffraction pattern to previously proposed hexagonal graphitic models for C_3N_4. Instead, they proposed an alternate graphitic-like structure, involving a different ordering scheme of the carbon vacancies with an orthorhombic unit cell. However, to obtain a more reliable structural characterization, a higher degree of crystallinity would be necessary. Chemical analysis indicates that the material synthesized by Alves et al.[24] also contained a significant fraction of hydrogen with a bulk stoichiometry of approximately $C_3N_4H_2$.

In this work we report the bulk synthesis of a well-crystallized material containing an extended network of alternating carbon and nitrogen atoms, with a network stoichiometry close to C_3N_4. The new compound was synthesized at high pressures and moderate temperatures in a piston cylinder apparatus from solid-state reactions involving triazine-based molecular precursors. The stoichiometry is $C_6N_9H_4Cl$ as determined from bulk chemical analyses and from parallel electron energy loss (PEELS) spectroscopy in the electron microscope. All 13 observed diffraction lines can be indexed to a hexagonal cell with $a = 8.4379(10)$ Å and $c = 6.4296(2)$ Å. Systematic absences indicate a $P6_3/m$ space group. Our best structural model, consistent with the experimental data and chemical considerations, is a compound structurally related to the hexagonal graphitic model proposed by Kouvetakis et al.[20] but with one-third of the C_3N_3 triazine rings missing (see Figure 2). The resultant large voids in the graphene planes are occupied by chloride ions with an equivalent protonation of nitrogen sites on the framework. The infrared and ¹³C NMR spectra, as well as the density determined by pychnometry, are all consistent with this model structure and stoichiometry. Our work represents the first bulk synthesis of a well-characterized and highly crystalline material containing a continuous network of alternating C and N atoms. Similar reaction strategies are likely to produce a range of carbon nitride materials, some of which may prove to be useful precursors for the synthesis of dense low compressibility forms of C_3N_4.

Experimental Section

Synthesis Strategy for C_3N_4. In an attempt to synthesize a bulk extended solid form of C_3N_4, we employed a high-pressure "soft-chemistry" reaction strategy based on a metathesis polymerization of substituted triazine-based compounds. Two approaches were initially considered. The first can be described as the self-reaction of 2-amino-4,6-dichloro-1,3,5-triazine (ADCT) and is given by

$$n\text{C}_3\text{N}_4\text{H}_2\text{Cl}_2 \rightarrow n\text{C}_3\text{N}_4 + 2n\text{HCl} \qquad \text{(I)}$$

(15) Guo, L. P.; Chen., Y.; Wang, E. G.; Li, L.; Zhao, Z. X. *Chem. Phys. Lett.* **1997**, *268*, 26–30.

(16) Chowdhry, A. K. M. S.; Cameron, D. C.; Hashmi, M. S. J.; Gregg, J. M. *J. Mater. Res.* **1999**, *14*, 2359–2363.

(17) Martin-Gil, J.; Martin-Gil, F. J.; Sarikaya, M.; Qian, M.; Jose-Yacaman, M.; Rubio, A. *J. Appl. Phys.* **1997**, *81*, 2555–2559.

(18) He, D. W.; Zhang, F. X.; Zhang, X. Y.; Qin, Z. C.; Zhang, M.; Liu, R. P.; Xu, Y. F.; Wang, W. K. *J. Mater. Res.* **1998**, *13*, 3458–3462.

(19) Wang, J.; Lei, J.; Wang, R. *Phys. Rev. B* **1998**, *58*, 11890–11895.

(20) Kouvetakis, J.; Bandari, A.; Todd, M.; Wilkens, B.; Cave, N. *Chem. Mater.* **1994**, *6*, 811.

(21) Nesting, D. C.; Kouvetakis, J.; Badding, J. V. *The 5th NIRIM international Symposium on Advanced Materials (ISAM 1998)*; Tsukuba, Japan, 1998.

(22) Demazeau, G.; Montigaud, H.; Tanguy, B.; Birot, M.; Dunogues, J. *Rev. High Pressure Sci. Technol.* **1998**, *7*, 1345.
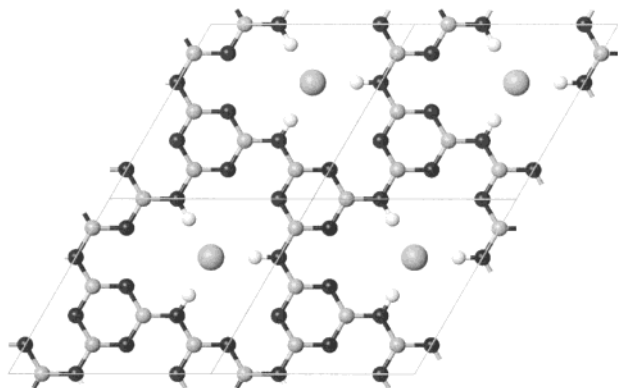
(23) Montigaud, H.; Tanguy B.; Demazeau, G.; Courjault, S.; Birot, M.; Dunogues, J. *C. R. Acad. Sci., Ser. IIb* **1997**, *325*, 229.

(24) Alves, I.; Demazeau, G.; Tanguy, B.; Weill, F. *Solid State Commun.* **1999**, *109*, 697.

7790   *J. Am. Chem. Soc., Vol. 123, No. 32, 2001*

Zhang et al.

reaction	precursors	P/T conditions
I	aminodichlorotriazine	1−1.5 GPa/500−600 °C
II	1 melamine + 2 cyanuric chloride	1−1.5 GPa/500−600 °C
III	1 melamine + 1 cyanuric chloride	1−1.5 GPa/500−600 °C

Figure 2. Proposed structure for the new carbon nitride $C_6N_9H_3\cdot HCl$ compound. The parent $C_6N_9H_3$ framework is a planar $P6_3/m$ network of alternating C and N atoms derived from an interconnection of triazine rings through bridging imido groups. The small gray spheres represent carbon, small black spheres nitrogen, small white spheres hydrogen, and large gray spheres chlorine. In this structure, each imido group connects only two triazine rings in comparison to the hypothetical "fully dense" C_3N_4 graphitic model (Figure 1) where nitrido groups bridge three triazine rings. Each of the large 24-atom ring voids within the $C_6N_9H_3$ network layers is occupied by a chloride atom. (The charge compensating proton is not displayed in this figure.)

In the second approach, 2,4,6-triamino-1,3,5-triazine (melamine) and 2,4,6-trichloro-1,3,5-triazine (cyanuric chloride) are combined in a 1:2 ratio through the reaction:

$$nC_3N_6H_6 + 2nC_3N_3Cl_3 \rightarrow 3nC_3N_4 + 6nHCl \qquad (II)$$
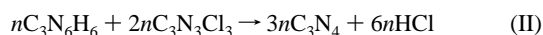
In both of these postulated reactions, the C_3N_3 heterocycle rings become linked via nitrido nitrogen atoms, through the elimination of HCl, to form extended graphene sheets of C_3N_4 composition. In such an idealized, "fully densified", C_3N_4 graphitic form, each nitrido group forms a link between three heterocycle rings (see also Figure 1). As discussed below, these condensation reactions can be favored over the competing decomposition reaction to graphite and nitrogen by carrying out the syntheses under high-pressure conditions ($P > 1$ GPa). We note that our reaction II strategy is similar to the reaction investigated by Demazeau et al.[22] except that these authors employed a solvothermal method at much lower pressures (150 MPa).

We performed a number of synthesis attempts of C_3N_4 using the above reaction strategies under various conditions of pressure and temperature. As discussed more completely below, we were not successful in obtaining the "fully dense" graphitic C_3N_4 material employing these methods. However, both reactions resulted in the formation of a novel carbon nitride phase that is structurally related to the hypothetical C_3N_4 graphitic phase. This novel compound possesses a carbon−nitrogen framework with stoichiometry $C_6N_9H_3$. The framework is best described as an open "graphene" C_3N_4 structure, in which one-third of the C_3N_3 triazine rings are missing (see Figure 2).

To optimize the formation and crystallization of this new phase we pursued a third reaction strategy (reaction III) whereby a 1:1 stoichiometric mixture of melamine with cyanuric chloride was combined via the reaction

$$nC_3N_6H_6 + nC_3N_3Cl_3 \rightarrow nC_6N_9H_3 + 3nHCl \qquad (III)$$
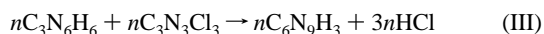
In this reaction, only two C_3N_3 heterocycle rings are linked by each imido group with the elimination of HCl to form a $C_6N_9H_3$ planar framework (see Figure 2). We find that, because the carbon nitride framework is strongly basic, it forms a 1:1 adduct with HCl under our synthetic conditions. This reaction and the product material are discussed more fully below.

Experimental Procedures. The melamine and cyanuric chloride precursor materials were obtained from Aldrich Chemical Co. and the 2-amino-4,6-dichloro-1,3,5-triazine (ADCT) was obtained from Monomer Polymer & Dajac Lab. All of these triazine-based compounds were

used as received. Because of the air and moisture sensitivity of these compounds, sample preparation and manipulation was performed under inert-atmosphere conditions using a drybox.

For all of the above reactions, approximately 250 mg of finely mixed powdered precursor(s) material was pressed into a 4.5 mm pellet. The pellet was then loaded into a platinum capsule (5 mm OD, 4.5 mm ID) and pressure-welded using a pellet press. The sample capsules were then removed from the drybox and placed in a non-end-loaded piston cylinder apparatus using a NaCl pressure transmitting medium. Each sample was held under a fixed temperature and pressure condition for 10 to 15 h. The sample capsules were then recovered and cut open in air. HCl emanated from the samples, indicating that polymerization had occurred. After the HCl was allowed to evaporate, the product was washed with water, followed by washes in ethanol and acetone. These washes removed a $Pt(NH_3)_4Cl_2$ phase that formed along the surface of the pellet due to a partial reaction of the reactants with the Pt capsule. Since the reactant materials are also partially soluble in water, the aqueous washes would have also removed any remaining nonpolymerized material. Samples I and III were then subjected to a heat treatment of 120 °C for about 10 h to remove residual H_2O.

Washed samples that were recovered from pressures between 1.0 and 1.5 GPa and temperatures between 500 and 600 °C were yellow in color and displayed the highest crystallinity with no evidence for decomposition to graphite. At temperatures above approximately 600 °C (at our typical synthesis pressures) some decomposition of the materials occurred as indicated by the presence of an insoluble carbon-rich graphitic material in the recovered samples. We report here the results of three synthesis reactions, based on the above strategies, where a highly crystalline nitrogen-rich material, closely related to the hypothetical C_3N_4 graphitic phase, was obtained.

For each of the three reactions studied, the precursor stoichiometric proportions and the pressure−temperature reaction conditions are listed in Table 1. In reaction I we investigated the self-reaction of 2-amino-4,6-dichloro-1,3,5-triazine (ADCT) whereas reactions II and III explored the reaction of melamine with cyanuric chloride in 1:2 and 1:1 stoichiometric proportions, respectively. Each of the reactions was duplicated several times.

Physical Measurements. X-ray powder diffraction data were obtained on samples dispersed with ethanol and deposited on a silica glass slide. Copper Kα radiation was used for the X-ray source and the diffraction data were collected with a Siemens D-5000 powder diffractometer using a position-sensitive detector, in Bragg-Bentano geometry. LeBail[25] and GSAS[26] refinements were made on the diffraction data using the program GSAS.

Parallel electron energy loss spectra of the product materials were acquired with a Gatan 666 EELS spectrometer attached to a Philips 400ST-FEG transmission electron microscope (TEM). The TEM was operated at 100 keV, with a probe semiangle of 0.9 mrad and a collection angle of 11 mrad. Under these conditions, the resolution of the TEM PEELS system was 0.9 eV. The spectrometer was calibrated against the boron K edge of hexagonal BN, which is at 192.14 eV.[27]

Core-loss edges were obtained from thin areas, typically <50 nm thick, overhanging holes in the lacy carbon film substrate. Spectra were acquired from areas of approximately 20 nm diameter in diffraction mode. The dark current and a background of the form AR^{-r} was subtracted from beneath each core-loss edge. The edges were further processed by deconvoluting the effect of the asymmetry of the zero-loss peak and the point spread function, following the procedures of

(25) LeBail, A.; Duroy, H.; Fourquet. J. L. *Mater. Res. Bull.* **1988**, *23*, 447−452.

(26) Larson, A. C.; Von Dreele, R. B. *General Structure Analysis System (GSAS)*, 1994.

(27) Garvie, L. A. J.; Craven, A. J.; Brydson, R. *Am. Mineral.* **1995**, *80*, 1132.

Table 2. Bulk Chemical Analyses of Reaction Products

reaction	bulk analysis (wt %)				total wt %	empirical formula
	C	N	Cl	H		
I	27.20	46.61	19.90	1.74	95.45	$C_6N_{8.82(\pm.09)}H_{4.57(\pm.66)}Cl_{1.49(\pm.02)}$
II	26.60	46.77	14.01	2.05	89.43	$C_6N_{9.05(\pm.09)}H_{5.51(\pm.67)}Cl_{1.07(\pm.02)}$
III	28.39	50.06	14.94	1.95	95.34	$C_6N_{9.07(\pm.09)}H_{4.91(\pm.63)}Cl_{1.07(\pm.02)}$

Egerton.[28] The PEELS spectra were analyzed with the Gatan el/p software and the elemental ratios determined using Hartree−Slater cross sections.

The PEELS spectra, acquired at an energy dispersion of 1 eV, span a sufficiently wide energy range to include the chlorine $L_{2,3}$ and the carbon, nitrogen, and oxygen K edges in the same spectrum, thus facilitating quantification. At least two spectra were acquired from each acquisition point; each spectrum was analyzed separately and their results averaged. The difference between the two sets of data from each analysis region was consistently less than ±10%.

Infrared transmission spectra were recorded with a Biorad FTS40 infrared spectrometer and MCT detector. The samples were prepared in pressed KBr pellets. Spectra were collected in the 4000 to 400 cm⁻¹ range with a resolution of 2 cm⁻¹.

The solid-state ¹³C NMR experiments were performed on a Varian UnityPlus 400 spectrometer using a multinuclear Varian 5 mm CP/MAS probe operating at 100.58 MHz. Samples were spun at 9 kHz in a silicon nitride rotor fitted with a torlon end cap. A variable-amplitude CP pulse sequence was employed and optimized at 9 kHz with hexamethylbenzene (HMB). Magic angle optimization was done with KBr, also at 9 kHz. Acquisition parameters included a 50 kHz sweep width, 3 s pulse delay, 3 ms 11-step contact time, and an applied line broadening of 200. Peak frequencies were calibrated using the methyl carbon of hexamethylbenzene as an external reference.

Pychnometric densities were measured on a Micrometrics AccuPyc-1330 pychnometer. Bulk elemental combustion analyses were obtained commercially from Desert Analytics Laboratory at the University of Arizona. For the elements reported, the confidence limits in the quoted weight percent quantities are ±0.25 wt %.

Results and Discussion

Compositional Analysis. Bulk elemental analyses (from C−N−H combustion) were performed on several batches of washed product derived from all three reactions. The average results are summarized in Table 2. The results of the bulk analyses for reactions II and III are very similar and indicate a C/N ratio near 6/9. The elemental analyses of all three products also indicate that a significant amount of Cl remains in the product. For products II and III, the relative abundance of chlorine is also approximately the same and the stoichiometric proportion of carbon, nitrogen, and chlorine is well described by the formula unit C_6N_9Cl. There is, however, a somewhat larger discrepancy in the relative abundance of hydrogen measured in the product materials.

As also indicated by the total weight percent in Table 2, there is a small residual of material not accounted for in the C−N−H−Cl combustion analysis for each sample. For reactions I and III this accounts for only 5 wt % of the samples, while for reaction II the residual is 10 wt %. H_2O is a likely candidate for some of this residual. This is especially true for reaction II since this sample was not heat treated after recovery and washing. Thermal gravimetric analysis on sample II indicated an initial 10−12 wt % loss on heating at 200 °C with minimal degradation of the sample crystallinity. Prolonged heating at this temperature resulted in a further gradual weight loss and partial degradation of the sample crystallinity as indicated by X-ray diffraction.
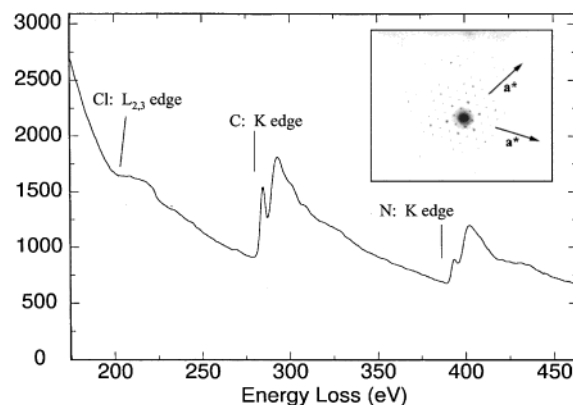
(28) Egerton, R. F. *Electron energy-loss spectroscopy in the electron microscope*; Plenum: New York, 1986.

Figure 3. Representative PEELS spectrum of a small grain in the washed product for reaction II. *K* electron excitations for C and N, and *L* electron excitations for Cl are observed in this energy loss region. Insert: Typical electron diffraction pattern taken from a thin flake. The measured *a* value from this pattern is 8.34 Å. The PEELS spectrum displayed here was taken on the same grain as that giving the electron diffraction pattern shown in the Figure 3 inset.

Electron Diffraction and Energy Loss Spectroscopy. Selective area electron diffration and parallel electron energy loss (PEELS) spectroscopy were performed within the electron microscope on several grains of the product material obtained from reaction II. Most all of the grains examined were highly crystalline, although some amorphous grains were also observed. Prolonged electron irradiation degraded the sample crystallinity.

The electron diffraction pattern of a small crystalline flake (<20 nm) is shown as an insert in Figure 3. In this zone, the electron diffraction pattern displays a hexagonal pattern with a basal unit cell parameter of $a = 8.34(5)$ Å. This value is consistent with d spacing measurements obtained from the X-ray diffraction measurements discussed below.

A representative low-resolution PEELS spectrum from sample II is also shown in Figure 3. The PEELS spectrum displayed here was taken on the same grain as that giving the electron diffraction pattern shown in the Figure 3 inset. The spectrum shows intense carbon and nitrogen *K* edges and a weaker chlorine $L_{2,3}$ edge. Quantitative analyses gives a C:N ratio of about 1:1.4 for all particles analyzed. Differences between analyses from the same particle were less than ±10% for C and N. A larger grain-to-grain variation was found for chlorine. This variation was due to the difficulty of quantifying the weaker Cl $L_{2,3}$ edge, and the loss of Cl under the electron beam. An elemental ratio (normalized to carbon) of $C_6N_{8.2(\pm0.4)}Cl_{0.8(\pm0.2)}$ was obtained by averaging results from four different particles. This stoichiometry is in good agreement with the results of the bulk chemical analyses. Since all of the grains characterized with PEELS gave a very similar C:N ratio, which is consistent with that obtained from the bulk chemical analysis, these observations provide supporting evidence that the product material is single phase. We also note that the oxygen abundance was below the detection limit in the EELS measurements indicating that there is no structural oxygen in the compound; any weakly bound H_2O would have likely been removed under
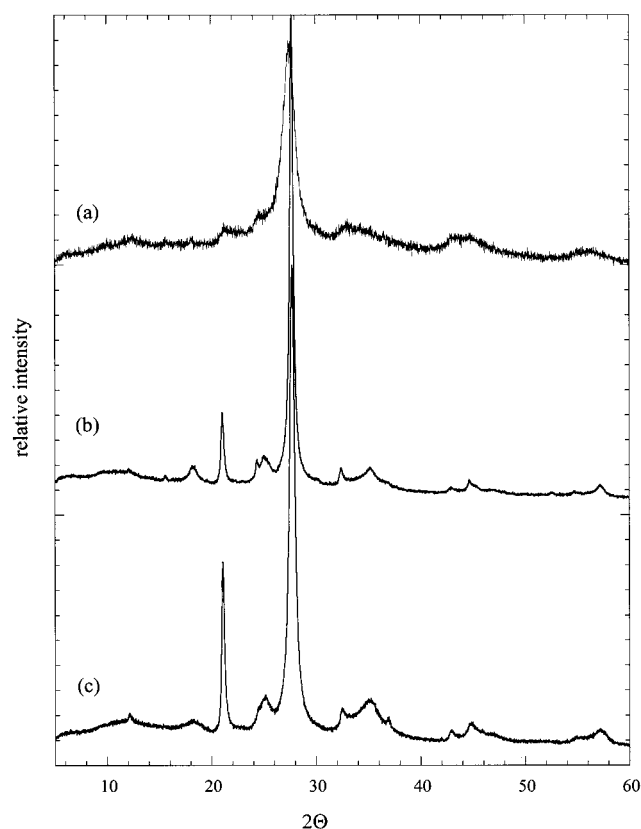
Figure 4. X-ray diffraction pattern of washed product for (a) reaction I, (b) reaction II, and (c) reaction III. The spectrum was collected using copper Kα radiation.

the electron beam irradiation and the high vacuum conditions of the electron microscope.

More detailed analyses of the PEELS spectra indicate that the first near-edge structure peak of C and N is attributed to transitions of the core 1s electrons to states with π^* symmetry and is indicative of sp^2 bonding.[29] The close similarities between the carbon and nitrogen K edges are indicative of strong covalent bonding between C and N. Moreover, the carbon and nitrogen π^* peaks also exhibit orientation-dependent intensity changes and the concomitant orientation effects of their K edges indicate similar anisotropic bonding sites for C and N. With an electron probe parallel to the hexagonal c-axis (e$^-$ || c-axis) more excitations into states of σ character are detected than into states of π character, whereas a probe perpendicular to the c-axis (e$^-$ ⊥ c-axis) results in detection of similar numbers of excitations into states of each character, with resulting higher π^* peak intensity.

X-ray Diffraction and Structure Refinement. The X-ray diffraction patterns of the washed products of reactions I, II, and III are shown in Figure 4. Although the diffraction patterns of the products are similar, those obtained from reactions II and III have narrower peaks, indicating a higher degree of crystallinity.

The X-ray diffraction spectra of the product material for all three reactions is characterized by a very strong reflection centered at 3.21 Å. This peak is reminiscent of the 002 basal plane reflection in graphite that occurs at 3.32 Å. A complete list of the diffraction peaks of the X-ray spectrum for the washed product of reaction II is given in Table 3. In addition to the strong reflection at 3.32 Å, a set of weaker lines occur in the

(29) Garvie, L. A. J.; Craven A. J.; Brydson R. *Am. Mineral.* **1994**, *79*, 411.

Table 3. Observed Peak Positions in $C_6N_9H_4Cl$

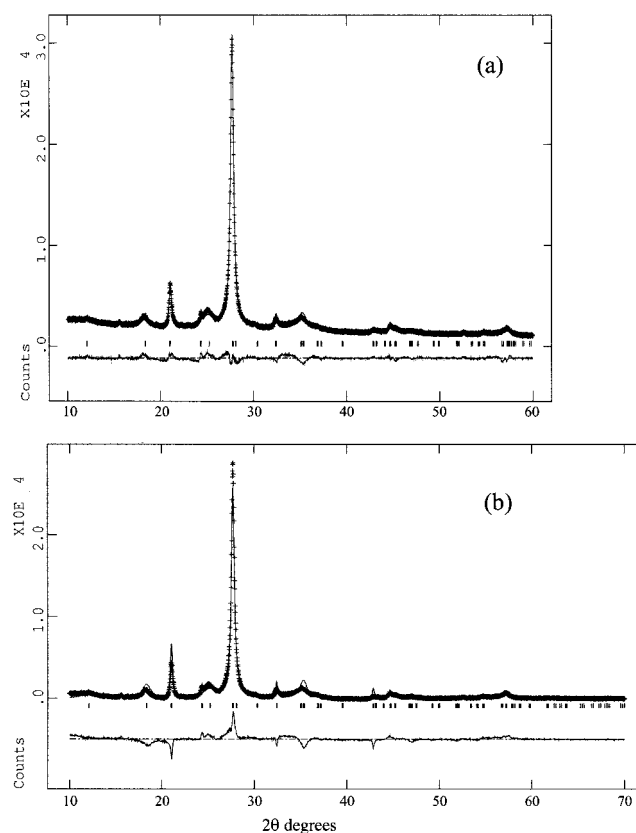| hkl	I(est.)	d_{obs}	d_{LeBail}
010	1	7.311	7.305
011	4	4.833	4.831
110	16	4.219	4.217
200	5	3.654	3.652
111	7	3.539	3.528
002	100	3.218	3.220
210	3	2.763	2.761
211, 112	5	2.546	2.537, 2.559
300	1	2.438	2.435
220	<1	2.106	2.108
130	3	2.027	2.026
023	<1	1.851	1.851
230	<1	1.678	1.676
004	3.9	1.609	1.610

Figure 5. (a) LeBail refinement of the X-ray diffraction data for the washed product of reaction II. (b) Rietveld refinement of the X-ray diffraction data for the washed product of reaction II. Difference plots (data − model) are provided for each fit. Measured data are indicated by crosses and the refined fit models are given as solid lines.

spectrum which obey the planar hexagonal relationship $1/d^2 = (4/3a^2)^*(1, 3, 4, 7, 9, 13, ...)$, with $a = 8.44(1)$ Å. The diffraction data strongly indicate the presence of ordering in the basal plane of the material, with a unit cell that is a supercell of graphite. In fact, the observed value of a is only slightly less than $2\sqrt{3}$ times the basal cell parameter of the hexagonal graphite phase (for graphite, $2\sqrt{3}a = 8.507$ Å). Because of the systematic absences that occur for the 001 and 003 reflections, the observed hexagonal diffraction pattern is consistent with a $P6_3/m$ space group.

Le Bail extraction[25] was used to determine the unit cell parameters and study peak shapes (Figure 5a). The peak shapes exhibit a significant degree of anisotropy and could be reasonably fit using Lorentzian parameters that depended on the crystallographic direction. Using this extraction method, hex-

*High-Pressure Bulk Synthesis of Crystalline C₆N₉H₃·HCl*High-Pressure Bulk Synthesis of Crystalline $C_6N_9H_3 \cdot HCl$

J. Am. Chem. Soc., Vol. 123, No. 32, 2001 7793

Table 4. Atomic Positions for $C_6N_9H_4Cl$ in the Ideal Structure ($P6_3/m$, $a = 8.4352(8)$ Å and $c = 6.4403(1)$ Å)

atom	site	x	y	z
Cl	2c	1/3	2/3	1/4
N(1)	6h	0	5/6	1/4
N(2)	6h	0	1/3	1/4
N(3)	6h	1/2	1/3	1/4
C(1)	6h	0	1/6	1/4
C(2)	6h	1/2	1/6	1/4

agonal cell parameters of $a = 8.4379(10)$ Å and $c = 6.4296(2)$ Å were obtained in the $P6_3/m$ space group.

One model that is generally consistent with the chemical analysis, PEELS, X-ray, and spectroscopic data (discussed more fully below) is the layered structure shown in Figure 2 with composition $C_6N_9H_4Cl$ (we also write this as $C_6N_9H_3 \cdot HCl$). The hydrogen atom on the bridging imido group is directed toward the void. The large voids are hexagonally ordered giving a basal cell parameter that is approximately $\sqrt{3}$ times larger than that of the hypothetical fully densified C_3N_4 graphitic model (which is in turn twice as large as the primitive a parameter of graphite).

We find from chemical analysis that our product material contains approximately one HCl component for each $C_6N_9H_3$ unit. This ratio is precisely obtained if a single HCl unit is associated with every 24-atom void. Because the $C_6N_9H_3$ framework is a Lewis base, it is unlikely that molecular HCl species occupy these voids. Instead, the HCl molecules are likely dissociated such that each of the large voids in the graphene sheets is occupied by a single chloride ion with the equivalent H^+ ion protonating the C−N framework. From the X-ray data alone, it is not possible to constrain the hydrogen atom positions. However, some insights into the proton position are obtained from the spectroscopic data which we discuss more fully below.

Further confirmation of the proposed chemical formula and structure was made by pychnometric density measurements of the bulk sample (derived from reaction II). These measurements gave an average value of 1.98 ± 0.02 g/cm³. This value is nearly identical to the theoretical density of 1.99 g/cm³ for our $P6_3/m$ model $C_6N_9H_3 \cdot HCl$ phase. By comparison, the hypothetical fully densified C_3N_4 graphitic model (Figure 1) gives a theoretical density of 2.31 g/cm³ if our same lattice parameters are used.

Our best Rietveld refinement of the X-ray diffraction data using the proposed structure (hydrogen atoms not included) gave values of $wR_p = 14\%$ and $\chi^2 = 40$ (Figure 5b). The atom positions were fixed in their ideal positions (Table 4) and only the lattice parameters, background, and peak profiles were allowed to vary. The quality of our X-ray powder data was not sufficient to allow a complete refinement of the atomic positions. The Rietveld analysis gave an unusually large thermal parameter for the chlorine atom, indicating that positional disordering of the chlorine atom could be present. Refinements that allowed the chlorine atoms to move off of the 6h site did not give a significant improvement in the fit. As is common in graphitic materials, the carbon nitride phase may also display stacking disorder, or polytypism, either of which would also contribute to the difficulty in the structure refinement. Further improvements in the refinement could also possibly be made by allowing a concerted rotation of the triazine rings. However, this level of refinement could not be justifed from the present quality of our X-ray data.

Within our limited refinement of the structure, the C−N bond lengths cannot be unambiguously determined. However, if we assume that all of the C−N bond lengths are equal and that the C−N−C angle of the bridging amine groups is 120° (as is the case in the fully densified graphitic phase model, Figure 1),

the average C−N bond length derived from our measured basal lattice parameter is 1.406 Å. This value is only 0.012 Å shorter than the 1.418 Å C−C bond length in hexagonal graphite. However, on the basis of Slater's covalent atomic radii, it is expected that the average C−N bond length in sp² hybridized compounds should be about 0.05 Å shorter than the C−C bond length. This expectation is also consistent with first principles calculations on fully densified graphitic C_3N_4 structures where the predicted C−N bond length is between 1.35 and 1.38 Å for the equilibrated static lattice at zero pressure.[3−6] If we assume that the average C−N bond length in the product material is in fact 1.37 Å, the expanded cell parameter observed for the $P6_3/m$ phase can be accounted for by a concerted in-plane rotation of the triazine rings. A concerted planar rotation of the triazine rings would still maintain the $P6_3/m$ symmetry. A C−N−C bridging angle (between triazene rings) of only about 125.5° would be required to match the measured cell parameters. Since the size of the large 24-atom ring void is very sensitive to the value of the bridging angle, this additional structural degree of freedom in the CN framework may be important to accommodate guest molecules of varying size.

An interesting comparison can be made between this structure and that found for the triaminoguanidine hydrochloride.[30] Although this compound crystallizes as a molecular solid and not as a continuous sheet, the structure consists of a layered hexagonal ordering of triaminoguanidine (CN_6H_8) molecules with chloride ions centered in planar voids. In this molecular solid, the shortest distance between Cl and N is 3.19 Å. By comparison, the nonbonded Cl−N distance for our idealized $P6_3/m$ structure of $C_6N_9H_4Cl$ (Figure 2 and Table 4) is 2.81 Å. This distance would increase to 2.92 Å if the C−N−C bridging angle was 125.5°. This distance is still relatively short, but within the range of that observed for materials with hydrogen bonded N−H···Cl groups. As a further comparison, the interlayer spacing between the planar layers in triaminoguanidine hydrochloride is 3.126 Å, only slightly shorter than the interlayer spacing of 3.22 Å obtained for $[C_6N_9H_4]^+Cl^-$.

It is important to mention that further confirmation of the proposed continuous graphitic C−N network for our carbon nitride product comes from our in situ high-pressure compressibility measurements.[31] If the carbon nitride material did not have a continuous framework structure it would possess a very large compressibility in all directions. On the contrary, we find that, like graphite, the compressibility of the basal plane of the carbon nitride product material is extremely low. Moreover, like graphite, the compressibility is highly anisotropic: in the a direction the compressibility is very low, and only slightly greater than that of graphite, while the compressibility along the c direction is very high and also comparable to that of graphite. The somewhat greater compressibility of the a parameter of the carbon nitride material relative to graphite can also be accommodated by including the rotational degree of freedom of the C_3N_3 heterocycles in the proposed C−N graphitic material, a compression mechanism that does not exist in the fully densified graphitic structure. A detailed study of the high-pressure and compressional behavior of this material will be presented elsewhere.[31]

Infrared Spectroscopic Characterization. Additional confirmation for the proposed graphitic-like structure of the product carbon nitride material and insight into the hydrogen atom locations can be obtained from the infrared and ^{13}C NMR spectra. The infrared transmission spectrum of a washed product

(30) Okaya, Y.; Pepinski, R. *Acta Crystallogr.* **1957**, *10*, 681.
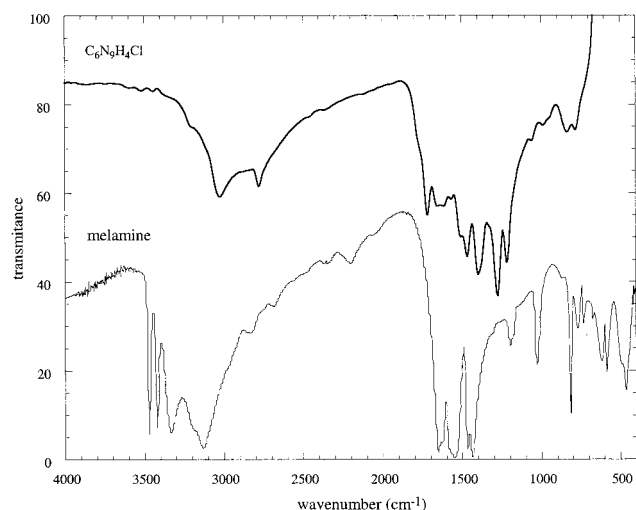(31) Bauer, M.; Wolf, G. H. In preparation.

7794   *J. Am. Chem. Soc., Vol. 123, No. 32, 2001*

Zhang et al.

Figure 6. Midinfrared transmission spectra of (a) carbon nitride product obtained from reaction III and (b) melamine spectra obtained from samples in a KBr pellet.

sample made through reaction III is shown in Figure 6. For comparison, we have also included the vibrational spectrum of melamine.

The infrared spectra of both melamine and the product material are characterized by several strong bands near 3000 cm^{-1} and a series of bands in the 1200–1600 cm^{-1} region. The bands near 3000 cm^{-1} are consistent with modes involving N–H stretching vibrations while the bands observed in the 1200–1600 cm^{-1} region are typical for molecules that contain CN heterocycles and are generally associated with the skeletal stretching vibrations of these aromatic rings.[32] Bending vibrations of terminal –NH$_2$ groups, as in melamine, also occur near 1600 cm^{-1}.

In melamine, the high-frequency modes above 3000 cm^{-1} can be assigned to the symmetric and antisymmetric stretching vibrations of the terminal NH$_2$ groups. The sharp bands that occur in melamine above 3300 cm^{-1} are associated with stretching modes involving hydrogen atoms that are not hydrogen bonded, while the lower frequency modes near 3100 cm^{-1} are much broader and associated with N–H stretching vibrations involving hydrogen-bonded units.

For the product material, the symmetric and antisymmetric –NH$_2$ stretching modes in the high-frequency region are missing. Instead, two broad infrared bands are observed at lower frequencies near 3024 and 2778 cm^{-1}. These bands likely represent vibrations involving N–H units. Within the hypothetical parent C$_6$N$_9$H$_3$ framework, all of the N–H groups possess the same local structure. Since there is little coupling between these units only a single unresolved N–H stretching vibrational band would be expected. The vibrational band at 3024 cm^{-1} is consistent with the stretching mode of the N–H nitrido groups bridging the C$_3$N$_3$ rings. Although the hydrogen stretching mode for neutral R$_2$N–H groups generally occurs at slightly higher frequencies,[32] hydrogen bonding interactions with the chloride ion, R$_2$N–H$\cdots$Cl$^-$, could lower the frequency of this mode.

Additional N–H species will also be formed through the protonation of the C$_6$N$_9$H$_3$ network. In our proposed [C$_6$N$_9$H$_4$]$^+$-Cl$^-$ structure, each large void is occupied by a chloride ion with the charge compensating hydrogen ion protonating the network. The C$_6$N$_9$H$_3$ framework possesses two structurally

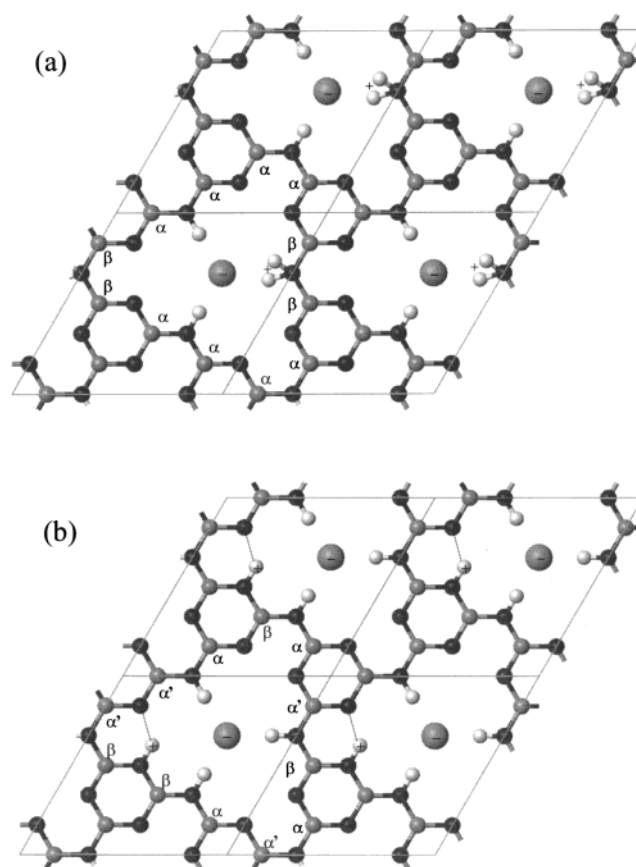(32) Katritzky, A. R.; Ambler, A. P. *Physical Methods in Heterocyclic Chemistry*; Katritzky, A. R., Ed.; Academic Press: New York and London, 1963; Vol. II, p 161.


Figure 7. Proposed structure models for charge-compensated [C$_6$N$_9$H$_4$]$^+$Cl$^-$. (a) In this model structure the proton is bound to an imide nitrogen atom. The 12 carbon atoms surrounding the large void are split into two chemically inequivalent carbon sites: 8 α and 4 β. The α carbon is bonded to two nitogen atoms contained within C$_3$N$_3$ heterocycles and to an imide nitrogen. For the β site, the carbon atom is also bonded to two nitrogen atoms contained within C$_3$N$_3$ heterocycles and the imide nitrogen that is also bonded to the charge compensating proton. (b) In this model the proton resides on a site where it is axially bonded to a nitrogen atom on a C$_3$N$_3$ heterocycle. In this proposed structure the 12 carbon atoms surrounding the large void are split into three structurally inequivalent carbon sites: 4 α, 4 α', and 4 β. The α and α' carbon sites have a similar first and second neighbor bonding arrangement except that for the α' site one of the heterocycle nitrogen atoms bonded to the carbon is also hydrogen bonded to the charge compensated proton. In the β carbon sites one of the heterocycle nitrogen atoms bonded to the carbon is also directly bonded to the charge compensating proton.

distinct proton acceptor nitrogen sites: the imido N–H groups that link the C$_3$N$_3$ heterocycles and the nitrogen atoms within these heterocycles. If only one or the other of these sites is protonated throughout the lattice, and the protons are ordered, two resultant structures can be obtained (Figure 7). Both structures possess the same carbon nitride framework and would not be distinguishable from our X-ray diffraction measurements.

In the case where the bridging imide group is protonated (Figure 7a), a R$_2$NH$_2$$^+$ species is formed. In this structure, the bridging nitrogen atom becomes sp^3 hybridized and any extended π-electron conjugation is disrupted. Conversely, if the hydrogen ion protonates the axial lone pair electrons of the nitrogen atom within the C$_3$N$_3$ heterocycle (Figure 7b), the nitrogen hybridization remains sp^2 and there is no disruption of the π-electron resonance configurations. Further stabilization of this protonated structure could also occur through a hydrogen-bonding interaction with the nitrogen atom on an adjacent
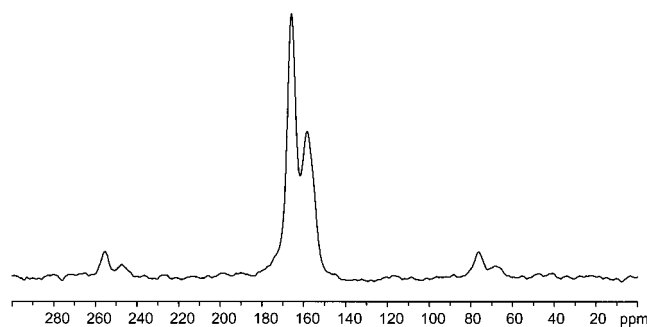
Figure 8. ^{13}C CP/MAS NMR spectrum of sample from reaction II. Chemical shifts are relative to HMB. Spinning sidebands also occur and are shifted approximately 90 ppm from the center bands.

heterocycle. The unusually low N—H stretching frequency observed for the product material at 2778 cm^{-1} would be consistent with the stretching vibration of a $R_2NH^+\cdots N$ unit (structure 7b).

^{13}C NMR Spectroscopic Characterization. The ^{13}C NMR spectrum of the product material of reaction III, obtained using proton cross-polarization, is shown in Figure 8. The spectrum consists of two major bands centered at about 166 and 159 ppm, referenced to HMB. The 159 ppm band has a weakly resolved shoulder at 156 ppm. A decomposition of the NMR spectrum yields a value of approximately 2:1 for the relative intensity ratio of the 166 and 159 ppm bands, respectively. Although cross-polarization experiments of these type are not always reliable for quantitative NMR analysis, two major resonance bands were also observed in a direct ^{13}C NMR spectrum. In these latter experiments, although the 156 ppm shoulder could not be resolved on account of the poor signal-to-noise ratio, consistent results for the intensity ratio of the two major bands were obtained.

The observed ^{13}C chemical shift values for the product material are typical for carbon sites in nitrogen-containing aromatic heterocycles.[33] The strong ^{13}C NMR peak observed at 166 ppm for the product material has a chemical shift that is very close to the 167.10 ppm value observed for melamine (dissolved in DMSO).[34]

The NMR spectrum for the product material suggests the existence of at least two chemically unique carbon atoms. In the idealized $C_6N_9H_3$ network, each of the carbon atoms possess the same local bonding environment: two bonds to nitogen atoms contained within C_3N_3 heterocycles and a third bond to a briging imide nitrogen. For a single isolated basal sheet of the hypothetical $C_6N_9H_3$ network, all of the carbon atoms would be structurally equivalent. This equivalency is removed within the $P6_3/m$ symmetry, due to the ABAB stacking giving rise to two structurally unique C_3N_3 rings. The rings located at the corners of the unit cell are stacked on top of each other (along the *c* axis) while the rings that are centered inside the unit cell are stacked such that the large Cl$^-$ containing voids are located above and below each ring. Although these two types of rings are structurally inequivalent, the local bonding arrangement about each carbon site is identical and hence is not expected to be sufficient to account for the observed splitting in the ^{13}C NMR spectrum. Moreover, the observed intensity ratio for the two bands is approximately 2:1 while an intensity ratio of 1:1 would be expected for any splitting resulting from the $P6_3/m$ stacking sequence.

More plausibly, the observed splitting in the ^{13}C spectrum arises from the partial protonation of the $C_6N_9H_3$ framework. In the structure shown in Figure 7a, the charge compensating proton is directly bonded to a bridging imide group. This protonation would lead to two chemically unique carbon sites. If we consider the 12 carbon atoms that surround a large void, the protonation shown in Figure 7a results in 8 α-type carbons and 4 β-type carbons. The α carbons are bonded to 2 unprotonated nitrogen atoms and 1 bridging NH group, whereas, the β-carbon is bonded to 2 unprotonated nitrogen atoms and 1 bridging NH_2^+ group. Hence, two peaks, with an intensity ratio of 2:1, would be predicted for the ^{13}C NMR spectrum of this hypothetical phase.

In the alternate structure shown in Figure 7b, a nitrogen atom within the C_3N_3 heterocycle is protonated. Here, the 12 carbon atoms surrounding the large void are split into three structurally inequivalent carbon sites: 4 α, 4 α′, and 4 β. The α carbons are each bonded to 2 unprotonated nitrogen atoms within C_3N_3 rings and 1 bridging NH group. The α′ carbon bonding environment is similar except that one of the ring nitrogen atoms bonded to the carbon is also hydrogen bonded to the charge compensating proton. For the β carbon, one of the heterocycle nitrogen atoms bonded to the carbon is also axially bonded to the charge compensating proton. If each of these carbon sites were resolved in the ^{13}C NMR spectrum, three peaks would occur with a 1:1:1 intensity ratio. We note, however, that the shielding environments of the α and α′ carbon sites are very similar and may not be resolved in an NMR spectrum. In this case, two bands would occur giving a 2:1 intensity ratio for the (α + α′) and β bands.

From our present data, we cannot unambiguously distinuish between these proposed structural models for the charge-compensated $[C_6N_9H_4]^+Cl^-$ material. However, a strong chemical argument can be made for the plausibility of the model shown in Figure 7b on the basis of the relative basicities of the aromatic and imide nitrogen centers in the $C_6N_9H_3$ framework. In comparisons to molecular organic systems,[35] the aromatic ring nitrogen atom in pyridine (pK_b 8.6) is only slightly more basic than the amino group in aniline (pK_b 9.4). However, the basicity of the amino group is markedly reduced when it is conjugated to two aromatic rings, e.g., diphenylamine has a pK_b of 13.2. In contrast, the basicity of the aromatic ring nitrogen is increased when it is ortho or para conjugated to an amino group, e.g., 4-pyridinamine has a pK_b of 4.86. Thus, within the $C_6N_9H_3$ framework, the nitrogen centers on the C_3N_3 heterocycles should be considerably more basic than the bridging imide nitrogen and would be preferentially protonated.

On this same note, we have also performed low-level Hartree—Fock electronic calculations on extended molecular clusters and these calculations do suggest that the structure shown in Figure 7b is energetically favored over the structure given in Figure 7a.

Conclusions

A new carbon nitride material with the stoichiometry $C_6N_9H_4$-Cl was prepared through a solid-state reaction of 2,4,6-triamino-1,3,5-triazine with 2,4,6-trichloro-1,3,5-triazine at 1.0—1.5 GPa and 500—550 °C. The yellowish compound crystallizes in a hexagonal space group ($P6_3/m$) with cell parameters of $a = 8.4379(10)$ Å and $c = 6.4296(2)$ Å with a pychnometric density of 1.99 g/cm^3. This new material possesses a two-dimensional $C_6N_9H_3$ network that is structurally related to the hypothetical

(33) Levy, G. C.; Lichter, R. L.; Nelson, G. L. *Carbon-13 Nuclear Resonance Spectroscopy*, 2nd ed.; John Wiley & Sons: New York, 1980.
(34) Pouchert, C. J. *The Aldrich Library of NMR Spectra*, 2nd ed.; Aldrich Chemical Co.: Milwaukee, WI, 1983.

(35) *Hanbook of Chemistry and Physics*, 79th ed.; Lide, D. R., Ed.; CRC Press LLC: Boca Raton, FL, 1998.

graphitic phase of C_3N_4. In this comparison, the new compound contains an ordered hexagonal arrangement of voids in the C−N graphitic framework but with one-third of the C_3N_3 heterocycles missing. The large voids in the graphene planes are occupied by chloride ions and the carbon nitride framework is protonated with an equivalent number of protons to maintain charge balance. On the basis of the infrared and ^{13}C NMR spectra, together with chemical considerations, we suggest that the hydrogen protonation occurs at the heterocycle nitrogen centers (Figure 7b), rather than at the imide nitrogen (Figure 7a). Moreover, the reduction of the Lewis basicity of the imide nitrogen in the $C_6N_9H_3$ network, arising from its conjugation with two aromatic heterocycle rings, may effectively reduce the reactivity of this site to further conjugation and hence may preclude the formation of an idealized fully densified C_3N_4 graphite using these reaction strategies. Modified synthetic strategies are currently being explored in our laboratory.

Most significantly, this work represents the first bulk synthesis of a well-characterized and highly crystalline material containing a continuous network of alternating C and N atoms. Similar reaction strategies are likely to produce a range of carbon nitride materials, some of which may prove to be useful precursors for the synthesis of dense low-compressibility forms of C_3N_4. Investigations into the ion exchange properties and the high-pressure behavior of this and similar graphitic carbon nitride materials will be presented elsewhere.